ChemPubSoc Europe

DOI: 10.1002/cphc.201300200

From Molecular Complexes to Complex Metallic Nanostructures—^{2}H Solid-State NMR Studies of Ruthenium-Containing Hydrogenation Catalysts

Torsten Gutmann,[a] Iker del Rosal,[b] Bruno Chaudret,[b] Romuald Poteau,[b] Hans-Heinrich Limbach,[a, c] and Gerd Buntkowsky*[a]

In the last years, the combination of ^{2}H solid-state NMR techniques with quantum-chemical calculations has evolved into a powerful spectroscopic tool for the characterization of the state of hydrogen on the surfaces of heterogeneous catalysts. In the present minireview, a brief summary of this development is given, in which investigations of the structure and dynamics of hydrogen in molecular complexes, clusters and nanoparticle systems are presented, aimed to understand the reaction mechanisms on the surface of hydrogenation catalysts. The surface state of deuterium/hydrogen is analyzed employing a combination of variable-temperature ^{2}H static and magic-angle spinning (MAS) solid-state NMR techniques, in which the dominant quadrupolar interactions of deuterium give information on the binding situation and local symmetry of deuterium/hydrogen on molecular species. Using a correlation database from molecular complexes and clusters, the possibility to distinguish between terminal Ru–D, bridged Ru_2–D, three-fold Ru_3–D, and interstitial Ru_6–D is demonstrated. Combining these results with quantum-chemical density functional theory (DFT) calculations allows the interpretation of ^{2}H solid-state data of complex "real world" nanostructures, which yielded new insights into reaction pathways at the molecular level.

1. Introduction

Hydrogen plays an important role in a number of catalytic reactions. Important technical processes such as Haber–Bosch,[1,2] Fischer–Tropsch,[3–5] or arene hydrogenation,[6–8] among others contain hydrogen conversion steps involving metal complexes or nanoparticles, which revolutionized the industrial production of basic chemicals and pushed forward the economy. Likewise, in the synthesis of pharmaceutical substances, the asymmetric hydrogenation of functional groups represents an important step to produce highly effective drugs, for example, L-DOPA, a therapeutic agent for Parkinson disease.[9,10] Thus, the detailed understanding of the catalytic pathways in hydrogenation reactions plays an essential role in the optimization of the aforementioned processes.

In the last years, hydrogen became also important as analytic probe, namely in the *para*-hydrogen induced polarization.[11,12] This technique is based on the nuclear spin polarization of the *para*-hydrogen spin isomer,[13,14] which can be used to increase the sensitivity of nuclear magnetic resonance (NMR) and magnetic resonance imaging (MRI).[15–18] The success of these experiments depends on the mechanism of the catalytic hydrogenation as well as on the *para-ortho* spin conversions occurring at the metallic centres.[19–25]

To get detailed knowledge on reaction processes taking place at the surface of catalysts, an extensive characterization of hydrogen binding and dynamics is important. For crystalline systems, it is possible to get precise information on hydrogen-binding geometries and distances, as well as on hydrogen dynamics, using inelastic neutron scattering (INS)[26–29] or surface-sensitive ultra-high vacuum techniques.[30–34] However, for complex non-ideal materials typically encountered in "real-world" experiments [e.g. non-crystalline metallic nanoparticles (MNPs) or carrier-supported heterogeneous catalysts], these techniques are less suitable and alternative techniques are needed to characterize the surface species. In recent years, solid-state NMR has evolved into such a characterization technique. For example ^{13}C and ^{31}P NMR has been well established to study the coordination of ligands at the surface of nanoparticles.[35–40] In particular, ^{13}C MAS and ^{13}C cross-polarization MAS (CP MAS) are able to characterize small probe molecules like CO adsorbed at the surfaces of MNPs,[38–44] and to distinguish between different CO binding geometries such as terminal, bridged, multicarbonyl, and strongly mobile CO (see Figure 1).

The investigation of hydrogen interacting with MNPs using ^{1}H solid-state NMR is more elaborate[45] due to usually strong proton background signals from the ligands at the surface and the presence of strong homonuclear proton–proton dipolar interactions. A typical example of these problems is shown in the work by Debouttière et al.,[46] in which the weak, tentative ^{1}H NMR signal of the hydride was so strongly overshadowed

[a] Dr. T. Gutmann, Prof. Dr. H.-H. Limbach, Prof. Dr. G. Buntkowsky
Eduard-Zintl Institut für physikalische und anorganische Chemie
Technische Universität Darmstadt
Petersenstraße 20, 64287 Darmstadt (Germany)
E-mail: gerd.buntkowsky@chemie.tu-darmstadt.de

[b] Dr. I. del Rosal, Dr. B. Chaudret, Prof. Dr. R. Poteau
Université de Toulouse; INSA, UPS, CNRS; LPCNO
135 Avenue de Rangueil, 31077 Toulouse (France)

[c] Prof. Dr. H.-H. Limbach
Institut für Chemie und Biochemie
Freie Universität Berlin
Takustraße 3, 17195 Berlin (Germany)

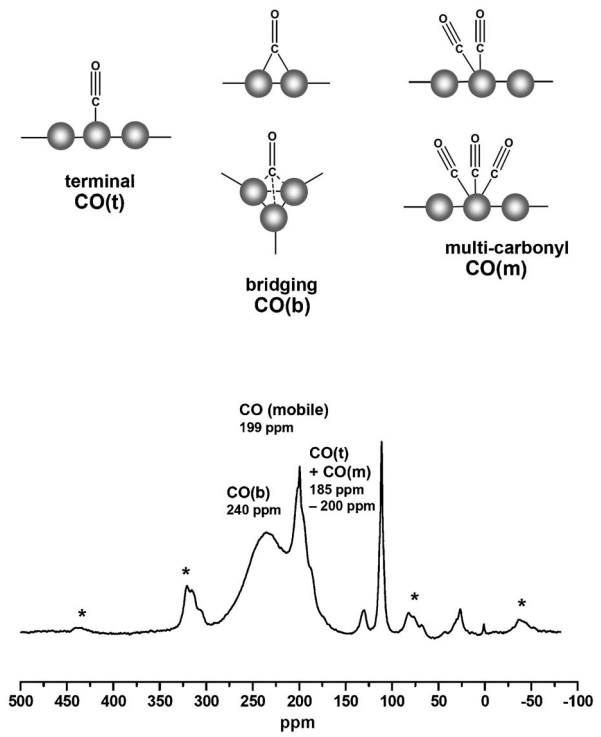

Figure 1. ^{13}C MAS NMR at 12 kHz spinning of Rudppb NPs containing co-adsorbed CO in different binding geometries.[44] From the analysis of the spectral lineshape it is possible to distinguish between terminal, bridging and multi-carbonyl (broad signals with corresponding spinning side bands) as well as mobile CO (sharp liquid-like signal containing no spinning sidebands). Note: Signals marked with * refer to spinning sidebands of the signals between $\delta = 185$–200 ppm. The signal at $\delta = 111$ ppm is caused by the teflon inlet of the rotor. Signals at $\delta = 129$ ppm and $\delta = 26$ ppm refer to the dppb ligand coordinated to NPs.

by the ligand background that a clear identification as a hydride species was not possible. In principle, these couplings could be suppressed by CRAMPS-type (combined rotation and multiple-pulse sequence)[47] experiments or fast MAS.[48,49] For example, the Pruski group demonstrated in a pioneering paper[50] that already at 40 kHz spinning frequency a CRAMPS-like resolution is achievable in mesoporous organic-inorganic hybrid materials, for which the dipolar linewidth was reduced by molecular dynamics. However, CRAMPS-type experiments are notoriously difficult to set up, demanding to perform, and not suitable as a routine technique in most NMR labs. Other complications arise for the application of fast ^1H MAS techniques, which is usually strongly hindered by the necessity to prevent air contact with the samples studied by sealing the MAS rotors, or by using sealed-Pyrex MAS rotor inserts. That may, however, create spinning instabilities and additional signals. Owing to these difficulties, up to now, the application of ^1H solid-state NMR for MNPs is limited to rare examples.[46]

Both the background signal and the homonuclear dipolar interaction problem can be avoided to a very large extent by the use of deuterium.[51,52] Deuterium is a quadrupolar nucleus with $I = 1$ and, therefore, the quadrupolar interaction (characterized by the quadrupolar coupling constant, Q_{cc}, and the asymmetry parameter, η_Q) in general dominates the ^2H solid-state NMR spectra. These two parameters give information on the binding mode and the local symmetry of surface deuterium/hydrogen. A further parameter called the isotropic chemical shift (δ_{iso}), can be extracted directly from ^2H MAS NMR spectra, and enables the characterization of deuterium/hydrogen chemical environments. In addition, variable-temperature ^2H solid-state NMR is a feasible tool to get information on dynamics and hydrogen motional modes, bound to a molecular species or adsorbed on a surface. The high potential for application of ^2H solid-state NMR was first realized by Davis[53] and Jelinski[54] in their pioneering works from the 70s and 80s, employing this method for the study of the dynamics of hydrocarbon chains and the local dynamics of biopolymers. Similar dynamic studies on ^2H NMR were also performed on small complexes in host–guest systems, as shown, for example, by Coutant et al.[55]

The present minireview focuses on recent developments of ^2H solid-state NMR investigations on hydrogen bindings and dynamics, starting from well-characterized metal complexes and clusters containing ruthenium, which are used to build a database of ^2H solid-state NMR parameters. The obtained database is then utilized for the interpretation of hydrogen-binding situations and reaction pathways at the surface of complex ruthenium nanostructures. To confirm the interpretation, some advanced density functional theory (DFT) calculations are presented.

2. Molecular Dihydrogen Complexes

Molecular dihydrogen complexes constitute an important group of compounds with many interesting properties and applications.[56,57] For example, they are used as model systems for technical hydrogen storage or as stable model compounds for the molecular states occurring in the process of hydrogen adsorption on a metal center, which is the key step in catalytic hydrogenations.[58–60]

Owing to this importance, the seminal discovery of the development of the first stable dihydrogen complexes by Kubas et al. in the early 80s[61] initiated substantial efforts resulting in the synthesis of a considerable number of dihydrogen complexes.[62] Detailed studies of the binding state of dihydrogen and reaction pathways in these complexes are summarized in refs. [63–67].

For their catalytic behavior, dynamics such as exchange and rotational motions play an important role. In the 80s and 90s, Eckert et al. investigated tunnel splitting of fast dihydrogen rotations using INS techniques.[68–70] Exchange couplings observed in the ^1H NMR spectra of transition metal hydrides were identified as rotational tunnel splittings, averaged over different rovibrational states.[65,66]

Advanced studies on the dynamics in these systems by ^2H solid-state NMR were started in the late 90s, which gave access to slow dihydrogen dynamics. In a first step, the theory of incoherent and coherent (tunneling) hydrogen exchange was extended, employing the quantum-mechanical density matrix formalism,[71] from which simulations of the ^2H solid-state spectra lineshapes for these processes were performed.[65,72] These

primary theoretical results were used to analyze ^{2}H static NMR experiments at variable temperature for ionic transition-metal catalysts such as $[M(D_2)Cl(PPh_2CH_2CH_2PPh_2)_2]PF_6$ (M = Ru, Os),[73,74] which shed more light on tunneling and exchange phenomena. Furthermore, the neutral complexes $W(PCy_3)_2(CO)_3(D_2)$ and $Os(D_2)(Cl)_2(CO)(PiPr_3)$ were investigated, both experimentally and theoretically to look on D–D binding distances and tensor orientations.[75,76] These results formed the basis for a better understanding of hydrogen dynamics in molecular systems and helped to interpret the binding and dynamics of hydrogen in complex compounds and nanostructures.

3. Ruthenium Complexes and Cluster Compounds

Based on the results obtained for dihydrogen complexes, the analysis of binding and dynamics was extended to hydrogen-rich molecular systems, namely mononuclear ruthenium complexes containing both terminal Ru–H and Ru–H_2 species (Figure 2, **I**–**III**),[45,77–79] as well as multinuclear Ru cluster compounds containing bridged Ru_2–H, face-capped Ru_3–H, or interstitial Ru_6–H (Figure 2, **IV**–**VI**).[80,81]

Several Ru complexes were synthesized and their crystal structures were characterized employing X-ray and neutron-scattering techniques.[82–87] From these experiments, the hydrogen-binding situation was determined, forming the basis for the interpretation of solid-state NMR and theoretical studies, to be described in the following sections.

The prerequisite for experimental ^{2}H solid-state NMR investigations on these molecular systems was selective ^{2}H-labelling, which needed specific synthesis routes employing deuterated compounds, for example, heterogeneous gas–solid H_2/D_2-exchange experiments (for details, see refs. [79,81]). Spectra of mononuclear Ru complexes such as $RuD_2(D_2)_2(PCy_3)_2$ (**VII**, Figure 3a) were recorded under static conditions down to 10 K, at which temperature most deuterium dynamics are frozen.[79] In the case of multinuclear Ru complexes, ^{2}H MAS spectra were measured to extract δ_{iso} values next to the quadrupolar parameters Q_{cc} and η_Q (Figure 3c).[81] Static spectra were simulated employing a laboratory-written Matlab script based on the theory of solid-state NMR (Figure 3b),[88,89] which enabled the simultaneous fit of several Pake-like subspectra. The simulation of ^{2}H MAS spectra (Figure 3d) was performed with the Simpson software package.[90]

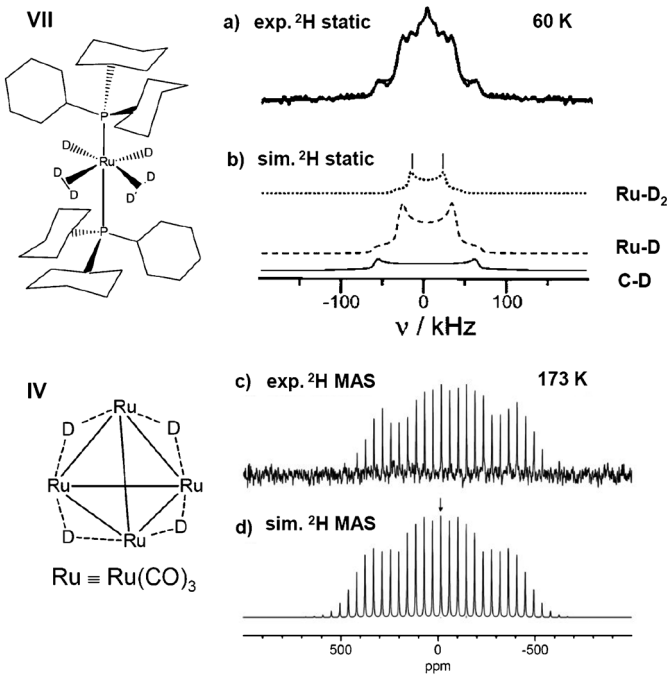

Figure 3. Upper panel: a) Experimental ^{2}H static NMR of $RuD_2(D_2)_2(PCy_3)_2$ (**VII**), and b) lineshape analysis of the ^{2}H static spectrum.[79] Lower panel: c) Experimental ^{2}H MAS NMR of $D_4Ru_4(CO)_{12}$ (**IV**) at 14 Tesla and 4 kHz spinning frequency, and d) simulated spectrum with $Q_{cc} = 67$ kHz and $\eta_Q = 0.67$, taken from ref. [81].

Parallel to this experimental work, DFT quantum-chemical calculations of the quadrupolar parameters were arranged for these model compounds at different levels of theory, namely at the B3PW91/cc-pVTZ or 6-31G(d,p) level for mononuclear complexes,[91] and at the B3LYP/6-31++G(d,p) level for cluster compounds.[81] Recently, the adsorption of hydrogen and its effect on the magnetic properties at small Ru_n cluster compounds was investigated by DFT methods.[92] In advanced theoretical studies, additional fictitious cluster compounds of Ru including different stabilizing ligand systems (CO, PH_3, PF_3, AsH_3,C_6H_6, etc.) were used to investigate the influence of the electronic environment on the NMR parameters,[93] and the ligand effect on NMR, vibrational and structural properties.[94]

The outcome of this combined ^{2}H NMR and DFT work is depicted in Table 1. It shows the typical range of experimental quadrupolar parameters ob-

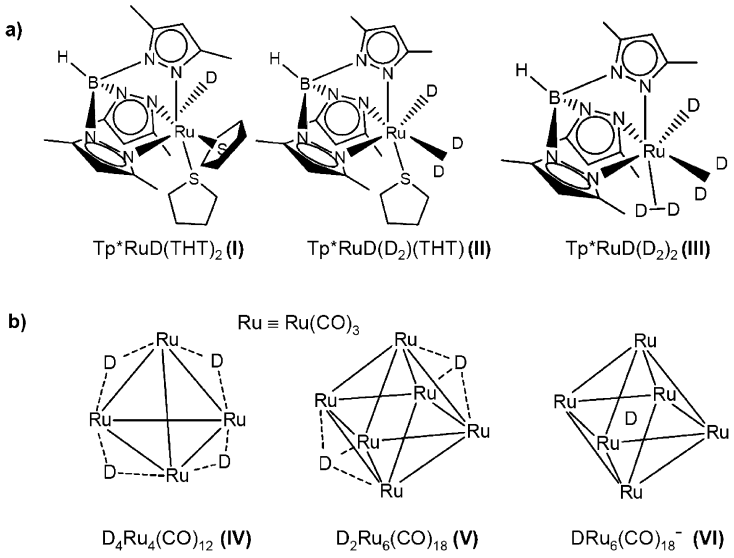

Figure 2. a) Model complexes,[79] and b) cluster compounds[81] for experimental ^{2}H solid-state NMR studies. These systems display examples for deuterium bound in different binding geometries, such as terminal, bridged, face-capped, and interstitial.

Table 1. Typical ^{2}H NMR parameters of deuterium bound to Ru in model complexes and clusters obtained from low-temperature static powder. MAS NMR experiments, and theoretical ^{2}H NMR parameters are based on DFT calculations. *n* number of model compounds for which experimental data were obtained; Q_{cc}, quadrupolar coupling constants; η_Q, asymmetry parameters; δ_{iso}, isotropic chemical shifts.

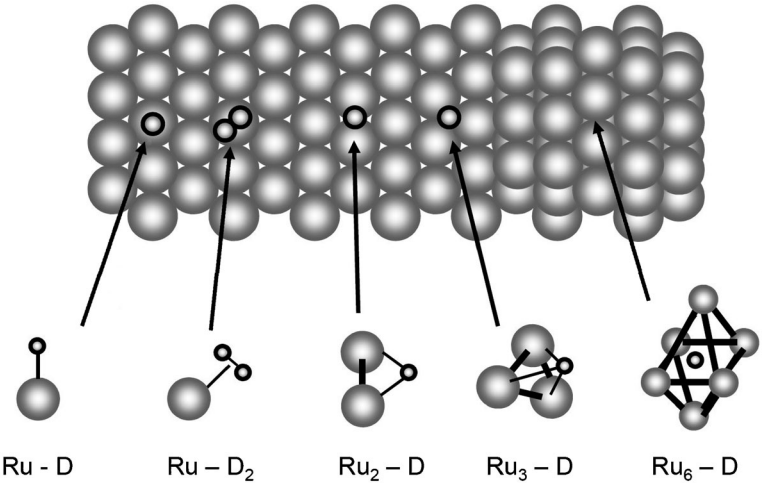

n	>3	>3	1	1	1
experimental ^{2}H NMR parameters for *n* model compounds[a]					
Q_{cc} [kHz]	80–100	50–80	≈70	≈25	≈0
η_Q	≈0	≈0	≈0.7	≈0.2	≈0
δ_{iso} [ppm]			≈−17	≈−16	≈+17
calculated ^{2}H NMR parameters for *n* model compounds					
Q_{cc} [kHz]	85–100[b]	70–100[b]	≈80[c]	≈35[c]	≈1[c]
η_Q	≈0–0.1[b]	≈0.1–1[b]	≈0.7[c]	≈0.3[c]	≈0
δ_{iso} [ppm]			≈−17[c]	≈−15.5[c]	≈+15.5[c]
calculated Q_{cc} values for a larger number of Ru complexes and clusters[d]					
Q_{cc} [kHz]	70–100	70–100	45–85	5–50	0–5

[a] Summarized experimental data from refs. [45,79,81]. [b] Calculated data at the B3PW91/cc-pVTZ level of theory from ref. [91]. [c] Calculated data at the B3LYP/6-31++G(d,p) level of theory from ref. [81]. [d] Calculated data for a variety of Ru complexes and clusters containing ligands with different steric and electronic properties at the B3PW91/cc-pVTZ level of theory from ref. [93].

tained from *n* model complexes, providing a comparison to the calculated range for these systems. In addition, a comparison with the parameter range for a larger number of fictional complexes is given. Both the experimental and the theoretical values are in good agreement and demonstrate that it is possible to distinguish clearly between bridged Ru_2–D, face-capped Ru_3–D, terminal Ru–D, and interstitial Ru_6–D by virtue of their ^{2}H quadrupolar interaction parameters.

The quadrupolar coupling constant, Q_{cc}, strongly depends on the local symmetry of the electric field at the deuterium position, and shows only a relatively weak dependency on the M–D bond length and ligand effect, as demonstrated by quantum-chemical calculations.[93] In particular, for an octahedral coordination (Ru_6–D) a Q_{cc} value equal to 0 kHz is observed, caused by the highly symmetric octahedral environment of the six Ru atoms, which yield an effective electric field gradient (EFG) of zero at the position of the central deuteron. Slight deviations from this high local symmetry result in a non-vanishing EFG, visible in the form of an increase of the Q_{cc} value. The second characteristic of the octahedrally coordinated deuterons is the strong low-field shift ($\delta = +17$ ppm) caused by the low-electron density of the deuterium environment, initiated by the surrounding Ru atoms. This shift is especially valuable to distinguish these deuterons from highly mobile deuterides, which are characterized by strong high-field shifts ($\delta = -16$ ppm and above).

For the signal assignment of terminal and face-capped (threefold) deuterides on the one hand, and bridged-coordinated deuterons on the other, the asymmetry parameter η_Q is useful, because it reflects the local binding geometry. For bridged deuterium atoms, a large η_Q value (>0.5) is expected, whereas for the highly symmetric threefold and terminal coordinations, a value close to zero (axial-symmetric) is assumed. In some cases, a deviation from η_Q is observed, which indicates mixed-binding states between bridged, threefold, and terminal coordination. Moreover, it is advisable to determine these parameters at temperatures low enough to exclude changes of the tensor symmetry by deuterium mobility.

A more complex situation is found for the coordination of $Ru–D_2$. Here, the lineshape of the NMR spectra is strongly influenced by dynamic effects, like deuterium mobility or deuterium exchange, which are not present in quantum-chemical calculations. In general, these effects cause both, a decrease of the experimental Q_{cc} value and a change of the experimental asymmetry parameter, compared to the values of a rigid system. These processes can be modelled by a combination of classical exchange-motions and tunnelling processes. While the classical exchange motions, characterized by an activation barrier, can be in principle completely suppressed by measuring at sufficiently low temperatures, the tunnelling motions occur even at very low values (for details see refs. [71,95]). A striking result of these motions is that, although the theoretically calculated η_Q values for $Ru–D_2$ are found close to one for a number of these model complexes, the experimentally determined asymmetry parameters are close to zero.[91] Thus, the experimental spectra clearly reveal the high dynamics of the dihydrogen systems, which are not completely frozen at the experimentally realizable temperature regions.

4. Ruthenium Nanoparticles

Parallel to the studies of molecular complexes the investigation of MNPs started. The particles were synthesized employing a new synthesis route working under mild conditions, which was developed by some of us.[96,97] As first model system Ru NPs were chosen to perform surface studies with ^{2}H solid-state NMR techniques. For such a system, the previously described correlation database was used to guide the interpretation of the spectra. Starting from well-defined Ru/hexadecylamine (HDA) NPs, in a first step, the presence of mobile surface hydrides in the particles was proven by Pery et al., employing a combination of ^{1}H gas-phase NMR experiments and ^{2}H solid-state NMR after a H_2/D_2-exchange reaction.[98] From the ^{2}H static NMR spectra it followed that not only surface hydrides were deuterated, but also nearby CH_2 groups from the ligands.

García-Antón et al. studied the hydrogenation of ethylene at the surface of Ru NPs using a simple model:[99]

$$C_2H_4 + D_2 \rightarrow C_2H_4D_2$$

Surprisingly, ^{2}H MAS NMR did not reveal only the presence of surface-bound deuterium, but also the presence of reaction intermediates in the form of surface-bound molecular fragments with deuterated methyl groups.

A second interesting example are the nanostructures of Ru particles embedded in a metal-organic framework (MOF).[100] In this system, the use of ^{2}H static NMR at variable temperatures between 23–200 K enabled the investigation of the hydride/deuteride dynamics. H/D exchange with the organic ligands was observed, indicated by a broad signal with $Q_{zz} = 130$–140 kHz, assignable to C–D groups in the ligand system. In addition, for this MOF D_2 ligands are localized, characterized by $Q_{zz} = 60$ kHz.

Further studies were performed on Ru NPs prepared inside SBA-3 silica materials and SBA-15 functionalized with carboxylic groups.[101]

The ^{2}H static NMR spectra of these nanomaterials were recorded after H/D-exchange experiments. Si–OD groups were detected showing the reactivity of the particles towards exchange reactions. In addition, the analysis of the particles spectra gave information on the deuteron-ruthenium binding situation on the surface. They indicate the presence of both dihydrogen (Ru–D_2) and monohydrogen [Ru_n–D ($n = 1,2,3,6$)] binding modes, characterized by their different quadrupolar couplings.

Very recently, surface chemistry ^{2}H NMR studies of Ru NPs stabilized by secondary phosphine oxides such as $OPH(PPh_3)_2$ were published.[37] This complex ligand system shows side reactions such as deuteration of the aromatic ring, as evidenced by IR (Figure 4, upper panel). Preliminary solid-state studies of these MNPs strongly indicate that the surrounding ligands form a hydrogen-bonding network, which may have an influence on the structure and reactivity of the particles for hydrogenation. ^{2}H static NMR measurements showed the binding situation of hydrogen in those complex nanostructures. O–D bonds next to C–D and Ru–D could be distinguished by the quadrupolar parameters (Figure 4, upper panel). These results were confirmed by MAS measurements, which revealed insights into the deuterons chemical environment, alongside variable-temperature ^{2}H solid-state NMR, used to monitor the mobility of the ligand system and surface hydrides.

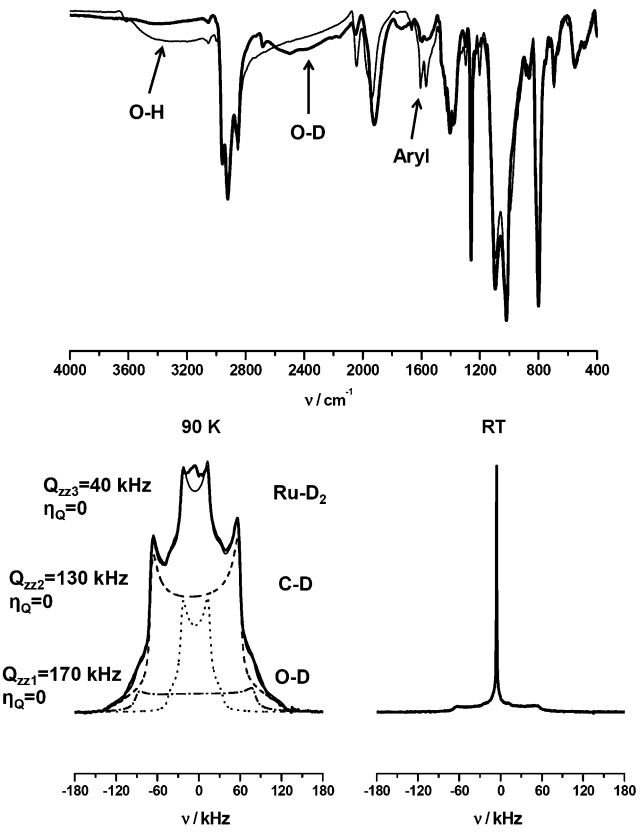

Figure 4. Upper panel: IR spectrum of $RuOPH(PPh_3)_2$ NPs before H/D exchange (—— and after H/D exchange (——). Lower panel: Comparison of the ^{2}H static NMR spectra of $RuOPH(PPh_3)_2$ NPs measured at 90 K and room temperature (RT), and lineshape analysis of the spectrum at 90 K. All spectra refer to ref. [37]

A deeper understanding of these experimental studies of deuterium on the surface of metal nanostructures necessitates theoretical modelling. Therefore, periodic-DFT calculations on an infinite Ru(0001) slab-surface model were performed recently.[102,103] Such model describes the more compact facets of Ru NPs. Although this model does not account for the edges, apexes, and other defects present in MNPs, it explains suitably the high density of states in large MNPs. In the calculations, a monolayer coverage value of 25% was first considered, a somewhat lower value compared to hydrogen-titration experiments for Ru NPs (1.1 H/surface Ru for Rudppb NPs, and 1.2 for RuPVP NPs).[44] These calculations confirmed that hydrogen preferably coordinates in threefold modes. Edge-bridging and on-top hydrogen atoms lie higher in energy, so that a large amount cannot be present on Ru(0001) surfaces. The coordination in six-fold or four-fold sites is much higher in energy, which reduces their probability of existence on the surface, independently of its coverage.

The quadrupolar parameters Q_{cc} and η_Q were calculated for all possible binding sites.[102,103] They show similar values com-

pared to those obtained from molecular complexes and clusters.[81,91,93] Interestingly, these parameters do not depend on the density of states, but rather on local symmetry. Thus, such quadrupolar fingerprints allow a safe assignment of experimental data obtained on Ru NPs.

From experimental data, the coexistence of on-top, edge-bridging, and face-capping hydrides at NPs surfaces is suggested, in contrast with the adsorption energies calculated on Ru(0001) slabs. This is not surprising if one takes into consideration that hcp Ru NPs are crystals with edges formed by several (hkl) facets (see Wulff construction, Figure 5, left panel).

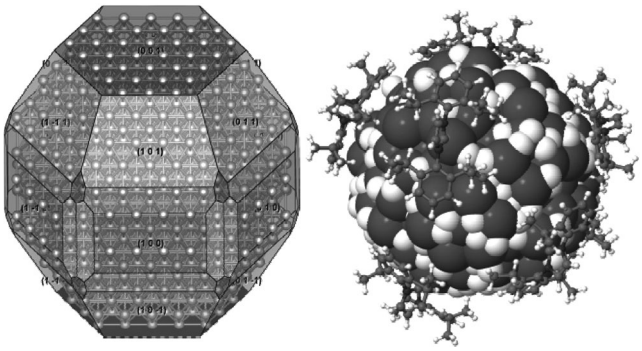

Figure 5. Left panel: Wulff construction of a bare 3 nm hcp Ru NP (adapted from ref. [104]). Right panel: Hypothetical geometry of a 1.8 nm hcp Ru NP, stabilized by 8 NHC ligands and accommodating 1.5 hydrides per surface Ru.[38]

Their surface topology is more diverse than a compact Ru(0001) plane, so that to some extent, it explains the variety of hydride coordination modes, together with their interaction with co-adsorbed ligands. A space-filling model of a 1.8 nm hcp Ru NP stabilized by N-heterocyclic carbene (NHC) ligands illustrates the richness of the surface chemistry of these species (Figure 5, right panel).

5. Summary and Outlook

In the present review we demonstrated that ^{2}H solid-state NMR spectroscopy combined with quantum-chemical calculations is a very useful technique with unprecedented power to characterize the binding situation of hydrogen in "real world" heterogeneous catalysts. Starting from the presented results on ruthenium NPs, research will be intensified in two different directions. First, a complete description of the solid-state spectra of Ru NPs will be developed, which includes also incoherent phenomena such as exchange or relaxation, which is crucial for the interpretation of the spectra lineshape at different temperatures. Next to the experimental part, research in the field of quantum-chemical calculations has to be intensified, employing larger model systems to look on hydrogen bindings, as well as on the influence of ligand systems on the organization of hydrogen at the surface of MNPs. Finally, dynamic phenomena, that is, adsorption, desorption, and diffusion of hydrogen/deuterium at the surface of nanostructures have to be taken into account to deliver a more complete understanding of surface processes, which are crucial for catalysis.

Acknowledgements

Financial support by the Agence nationale de la recherche and Deutsche Forschungsgemeinschaft in the framework of the ANR-11-INTB-1011 and DFG-911/19-1 MOCA-NANO project is gratefully acknowledged. The European Union is acknowledged for an European Research Council Advanced Grant 2009-246763. T.G. thanks the Centre national de la recherche scientifique–Max-Planck Gesellschaft cooperation for financial support for a post-doctoral stay in France.

Keywords: solid-state NMR · catalysis · density functional theory · nanoparticles · transition metal complexes

[1] G. Ertl, *Angew. Chem.* **1990**, *102*, 1258 – 1266; *Angew. Chem. Int. Ed. Engl.* **1990**, *29*, 1219 – 1227.
[2] R. Schlögl, *Angew. Chem.* **2003**, *115*, 2050 – 2055; *Angew. Chem. Int. Ed.* **2003**, *42*, 2004 – 2008.
[3] B. H. Davis, M. L. Occelli, *Fischer – Tropsch Synthesis, Catalysts and Catalysis*, Elsevier, Amsterdam, **2007**.
[4] C. X. Xiao, Z. P. Cai, T. Wang, Y. Kou, N. Yan, *Angew. Chem.* **2008**, *120*, 758 – 761; *Angew. Chem. Int. Ed.* **2008**, *47*, 746 – 749.
[5] S. Shetty, R. A. van Santen, *Catal. Today* **2011**, *171*, 168 – 173.
[6] A. Gual, M. R. Axet, K. Philippot, B. Chaudret, A. Denicourt-Nowicki, A. Roucoux, S. Castillon, C. Claver, *Chem. Commun.* **2008**, 2759 – 2761.
[7] X. Zhou, T. Wu, B. Hu, T. Jiang, B. Han, *J. Mol. Catal. A* **2009**, *306*, 143 – 148.
[8] A. Roucoux, C. Copéret, B. Chaudret in *Stabilized Noble Metal Nanoparticles: An Unavoidable Family of Catalysts for Arene Derivative Hydrogenation, Surface and Interfacial Organometallic Chemistry and Catalysis, Vol. 16*, Springer, Berlin/Heidelberg, **2005**, pp. 261 – 279.
[9] H. B. Kagan, *Pure Appl. Chem.* **1975**, *43*, 401 – 421.
[10] W. S. Knowles, *Acc. Chem. Res.* **1983**, *16*, 106 – 112.
[11] T. C. Eisenschmid, R. U. Kirss, P. P. Deutsch, S. I. Hommeltoft, R. Eisenberg, J. Bargon, R. G. Lawler, A. L. Balch, *J. Am. Chem. Soc.* **1987**, *109*, 8089 – 8091.
[12] J. Natterer, J. Bargon, *Prog. Nucl. Magn. Reson. Spectrosc.* **1997**, *31*, 293 – 315.
[13] C. R. Bowers, D. P. Weitekamp, *J. Am. Chem. Soc.* **1987**, *109*, 5541 – 5542.
[14] M. G. Pravica, D. P. Weitekamp, *Chem. Phys. Lett.* **1988**, *145*, 255 – 258.
[15] K. Golman, O. Axelsson, H. Johannesson, S. Mansson, C. Olofsson, J. S. Petersson, *Magn. Reson. Med.* **2001**, *46*, 1 – 5.
[16] S. B. Duckett, R. E. Mewis, *Acc. Chem. Res.* **2012**, *45*, 1247 – 1257.
[17] A. Viale, F. Reineri, D. Santelia, E. Cerutti, S. Ellena, R. Gobetto, S. Aime, *Q. J. Nucl. Med. Mol. Imag.* **2009**, *53*, 604 – 617.
[18] A. A. Lysova, I. V. Koptyug, *Chem. Soc. Rev.* **2010**, *39*, 4585 – 4601.
[19] G. Buntkowsky, J. Bargon, H. H. Limbach, *J. Am. Chem. Soc.* **1996**, *118*, 8677 – 8683.
[20] S. B. Duckett, C. J. Sleigh, *Prog. Nucl. Magn. Reson. Spectrosc.* **1999**, *34*, 71 – 92.
[21] S. B. Duckett, D. Blazina, *Eur. J. Inorg. Chem.* **2003**, 2901 – 2912.
[22] J. Matthes, T. Pery, S. Gründemann, G. Buntkowsky, S. Sabo-Etienne, B. Chaudret, H. H. Limbach, *J. Am. Chem. Soc.* **2004**, *126*, 8366 – 8367.
[23] G. Buntkowsky, B. Walaszek, A. Adamczyk, Y. Xu, H. H. Limbach, B. Chaudret, *Phys. Chem. Chem. Phys.* **2006**, *8*, 1929 – 1935.
[24] H. H. Limbach, G. Buntkowsky, J. Matthes, S. Gründemann, T. Pery, B. Walaszek, B. Chaudret, *ChemPhysChem* **2006**, *7*, 551 – 554.
[25] J. Matthes, S. Gründemann, G. Buntkowsky, B. Chaudret, H. H. Limbach, *Appl. Magn. Reson.* **2013**, *44*, 247 – 265.
[26] M. Grellier, L. Vendier, B. Chaudret, A. Albinati, S. Rizzato, S. Mason, S. Sabo-Etienne, *J. Am. Chem. Soc.* **2005**, *127*, 17592 – 17593.
[27] F. Fillaux, *Int. Rev. Phys. Chem.* **2000**, *19*, 553 – 564.

[28] P. W. Albers, S. F. Parker, *Adv. Catal.* **2007**, *51*, 99 – 132.
[29] S. Gründemann, H. H. Limbach, G. Buntkowsky, S. Sabo-Etienne, B. Chaudret, *J. Phys. Chem. A* **1999**, *103*, 4752 – 4754.
[30] G. Ertl, M. Huber, S. B. Lee, Z. Paal, M. Weiss, *Appl. Surf. Sci.* **1981**, *8*, 373 – 386.
[31] P. Feulner, D. Menzel, *Surf. Sci.* **1985**, *154*, 465 – 488.
[32] G. Lauth, E. Schwarz, K. Christmann, *J. Chem. Phys.* **1989**, *91*, 3729 – 3743.
[33] M. Sokolowski, T. Koch, H. Pfnur, *Surf. Sci.* **1991**, *243*, 261 – 272.
[34] G. A. Somorjai, G. Rupprechter, *J. Phys. Chem. B* **1999**, *103*, 1623 – 1638.
[35] R. Bronger, T. D. Le, S. Bastin, J. García-Antón, C. Citadelle, B. Chaudret, P. Lecante, A. Igau, K. Philippot, *New J. Chem.* **2011**, *35*, 2653 – 2660.
[36] D. González-Gálvez, P. Nolis, K. Philippot, B. Chaudret, P. W. N. M. van Leeuwen, *ACS Catal.* **2012**, *2*, 317 – 321.
[37] E. Rafter, T. Gutmann, F. Löw, G. Buntkowsky, K. Philippot, B. Chaudret, P. W. N. M. van Leeuwen, *Catal. Sci. Technol.* **2013**, *3*, 595 – 599.
[38] P. Lara, O. Rivada-Wheelaghan, S. Conejero, R. Poteau, K. Philippot, B. Chaudret, *Angew. Chem.* **2011**, *123*, 12286 – 12290; *Angew. Chem. Int. Ed.* **2011**, *50*, 12080 – 12084.
[39] P. Lara, M.-J. Casanove, P. Lecante, P.-F. Fazzini, K. Philippot, B. Chaudret, *J. Mater. Chem.* **2012**, *22*, 3578 – 3584.
[40] P. Lara, T. Ayvali, M.-J. Casanove, P. Lecante, A. Mayoral, P.-F. Fazzini, K. Philippot, B. Chaudret, *Dalton Trans.* **2013**, *42*, 372 – 382.
[41] T. M. Duncan, K. W. Zilm, D. M. Hamilton, T. W. Root, *J. Phys. Chem.* **1989**, *93*, 2583 – 2590.
[42] J. S. Bradley, J. M. Millar, E. W. Hill, S. Behal, B. Chaudret, A. Duteil, *Faraday Discuss.* **1991**, *92*, 255 – 268.
[43] K. Tedsree, A. T. S. Kong, S. C. Tsang, *Angew. Chem.* **2009**, *121*, 1471 – 1474; *Angew. Chem. Int. Ed.* **2009**, *48*, 1443 – 1446.
[44] F. Novio, K. Philippot, B. Chaudret, *Catal. Lett.* **2010**, *140*, 1 – 7.
[45] T. J. Geldbach, H. Rüeger, P. S. Pregosin, *Magn. Reson. Chem.* **2003**, *41*, 703 – 708.
[46] P.-J. Debouttière, Y. Coppel, A. Denicourt-Nowicki, A. Roucoux, B. Chaudret, K. Philippot, *Eur. J. Inorg. Chem.* **2012**, 1229 – 1236.
[47] B. C. Gerstein, R. G. Pembleton, R. C. Wilson, L. M. Ryan, *J. Chem. Phys.* **1977**, *66*, 361 – 362.
[48] L. S. Du, A. Samoson, T. Tuherm, C. P. Grey, *Chem. Mater.* **2000**, *12*, 3611 – 3616.
[49] A. Samoson in *Extended Magic-Angle Spinning, Vol. 9* (Eds.: D. M. Grant, R. K. Harris), Wiley, Chichester, **2002**, pp. 59 – 64.
[50] J. Trebosc, J. W. Wiench, S. Huh, V. S. Y. Lin, M. Pruski, *J. Am. Chem. Soc.* **2005**, *127*, 7587 – 7593.
[51] A. Grünberg, H. Breitzke, G. Buntkowsky in *Spectroscopic Properties of Inorganic and Organometallic Compounds: Techniques, Materials and Applications, Vol. 43*, Royal Chemical Society, London, **2012**, pp. 289 – 323.
[52] A. Adamczyk, Y. Xu, B. Walaszek, F. Roelofs, T. Pery, K. Pelzer, K. Philippot, B. Chaudret, H. H. Limbach, H. Breitzke, G. Buntkowsky, *Top. Catal.* **2008**, *48*, 75 – 83.
[53] J. H. Davis, K. R. Jeffrey, M. Bloom, M. I. Valic, *Chem. Phys. Lett.* **1976**, *42*, 390 – 394.
[54] L. W. Jelinski, *Ann. Rev. Mater. Sci.* **1985**, *15*, 359 – 377.
[55] M. A. Coutant, J. R. Sachleben, P. K. Dutta, *J. Phys. Chem. B* **2003**, *107*, 11000 – 11007.
[56] G. J. Kubas, *Catal. Lett.* **2005**, *104*, 79 – 101.
[57] R. H. Morris, *Coord. Chem. Rev.* **2008**, *252*, 2381 – 2394.
[58] G. Alcaraz, M. Grellier, S. Sabo-Etienne, *Acc. Chem. Res.* **2009**, *42*, 1640 – 1649.
[59] G. J. Kubas, *J. Organomet. Chem.* **2009**, *694*, 2648 – 2653.
[60] A. W. C. van den Berg, C. O. Arean, *Chem. Commun.* **2008**, 668 – 681.
[61] G. J. Kubas, R. R. Ryan, B. I. Swanson, P. J. Vergamini, H. J. Wasserman, *J. Am. Chem. Soc.* **1984**, *106*, 451 – 452.
[62] G. J. Kubas, *Metal Dihydrogen and Sigma-Bond Complexes*, Kluwer Academic/Plenum, New York, **2001**.
[63] P. G. Jessop, R. H. Morris, *Coord. Chem. Rev.* **1992**, *121*, 155 – 284.
[64] D. M. Heinekey, W. J. Oldham, *Chem. Rev.* **1993**, *93*, 913 – 926.
[65] H. H. Limbach, S. Ulrich, S. Gründemann, G. Buntkowsky, S. Sabo-Etienne, B. Chaudret, G. J. Kubas, J. Eckert, *J. Am. Chem. Soc.* **1998**, *120*, 7929 – 7943.
[66] H. H. Limbach, G. Scherer, M. Maurer, B. Chaudret, *Angew. Chem.* **1992**, *104*, 1414 – 1417; *Angew. Chem. Int. Ed. Engl.* **1992**, *31*, 1369 – 1372.
[67] G. J. Kubas, *Chem. Rev.* **2007**, *107*, 4152 – 4205.
[68] J. Eckert, G. J. Kubas, A. J. Dianoux, *J. Chem. Phys.* **1988**, *88*, 466 – 468.
[69] J. Eckert, *Spectrochim. Acta Part A* **1992**, *48*, 363 – 378.
[70] J. Eckert, G. J. Kubas, *J. Phys. Chem.* **1993**, *97*, 2378 – 2384.
[71] G. Buntkowsky, H. H. Limbach, *J. Low Temp. Phys.* **2006**, *143*, 55 – 114.
[72] G. Buntkowsky, H. H. Limbach, F. Wehrmann, I. Sack, H. M. Vieth, R. H. Morris, *J. Phys. Chem. A* **1997**, *101*, 4679 – 4689.
[73] F. Wehrmann, T. P. Fong, R. H. Morris, H. H. Limbach, G. Buntkowsky, *Phys. Chem. Chem. Phys.* **1999**, *1*, 4033 – 4041.
[74] G. A. Facey, T. P. Fong, D. Gusev, P. M. Macdonald, R. H. Morris, M. Schlaf, W. Xu, *Can. J. Chem.* **1999**, *77*, 1899 – 1910.
[75] G. Facey, D. Gusev, R. H. Morris, S. Macholl, G. Buntkowsky, *Phys. Chem. Chem. Phys.* **2000**, *2*, 935 – 941.
[76] F. Wehrmann, J. Albrecht, E. Gedat, G. J. Kubas, J. Eckert, H. H. Limbach, G. Buntkowsky, *J. Phys. Chem. A* **2002**, *106*, 2855 – 2861.
[77] V. Rodriguez, S. Sabo-Etienne, B. Chaudret, J. Thoburn, S. Ulrich, H. H. Limbach, J. Eckert, J. C. Barthelat, K. Hussein, C. J. Marsden, *Inorg. Chem.* **1998**, *37*, 3475 – 3485.
[78] S. Macholl, J. Matthes, H. H. Limbach, S. Sabo-Etienne, B. Chaudret, G. Buntkowsky, *Solid State Nucl. Magn. Reson.* **2009**, *36*, 137 – 143.
[79] B. Walaszek, A. Adamczyk, T. Pery, Y. P. Xu, T. Gutmann, N. D. Amadeu, S. Ulrich, H. Breitzke, H. M. Vieth, S. Sabo-Etienne, B. Chaudret, H. H. Limbach, G. Buntkowsky, *J. Am. Chem. Soc.* **2008**, *130*, 17502 – 17508.
[80] S. Aime, R. Gobetto, A. Orlandi, C. J. Groombridge, G. E. Hawkes, M. D. Mantle, K. D. Sales, *Organometallics* **1994**, *13*, 2375 – 2379.
[81] T. Gutmann, B. Walaszek, Y. P. Xu, M. Wächtler, I. del Rosal, A. Grünberg, R. Poteau, R. Axet, G. Lavigne, B. Chaudret, H. H. Limbach, G. Buntkowsky, *J. Am. Chem. Soc.* **2010**, *132*, 11759 – 11767.
[82] S. Sabo-Etienne, B. Chaudret, *Coord. Chem. Rev.* **1998**, *178*, 381 – 407.
[83] K. Hussein, C. J. Marsden, J. C. Barthelat, V. Rodríguez, S. Conejero, S. Sabo-Etienne, B. Donnadieu, B. Chaudret, *Chem. Commun.* **1999**, 1315 – 1316.
[84] A. F. Borowski, B. Donnadieu, J. C. Daran, S. Sabo-Etienne, B. Chaudret, *Chem. Commun.* **2000**, 543 – 544.
[85] A. J. Toner, S. Gründemann, E. Clot, H. H. Limbach, B. Donnadieu, S. Sabo-Etienne, B. Chaudret, *J. Am. Chem. Soc.* **2000**, *122*, 6777 – 6778.
[86] A. J. Toner, B. Donnadieu, S. Sabo-Etienne, B. Chaudret, X. Sava, F. Mathey, P. L. Floch, *Inorg. Chem.* **2001**, *40*, 3034 – 3038.
[87] J. Matthes, S. Gründemann, A. Toner, Y. Guari, B. Donnadieu, J. Spandl, S. Sabo-Etienne, E. Clot, H. H. Limbach, B. Chaudret, *Organometallics* **2004**, *23*, 1424 – 1433.
[88] K. Schmidt-Rohr, H. W. Spiess in *Principles of NMR of Organic Solids*, Academic Press, London, **1994**, pp. 13 – 68.
[89] C. P. Slichter, *Principles of Magnetic Resonance*, Springer, New York, **2000**.
[90] M. Bak, J. T. Rasmussen, N. C. Nielsen, *J. Magn. Reson.* **2000**, *147*, 296 – 330.
[91] I. del Rosal, T. Gutmann, L. Maron, F. Jolibois, B. Chaudret, B. Walaszek, H. H. Limbach, R. Poteau, G. Buntkowsky, *Phys. Chem. Chem. Phys.* **2009**, *11*, 5657 – 5663.
[92] G. X. Ge, H. X. Yan, Q. Jing, Y. H. Luo, *J. Cluster Sci.* **2011**, *22*, 473 – 489.
[93] I. del Rosal, T. Gutmann, B. Walaszek, I. C. Gerber, B. Chaudret, H. H. Limbach, G. Buntkowsky, R. Poteau, *Phys. Chem. Chem. Phys.* **2011**, *13*, 20199 – 20207.
[94] I. del Rosal, F. Jolibois, L. Maron, K. Philippot, B. Chaudret, R. Poteau, *Dalton Trans.* **2009**, 2142 – 2156.
[95] G. Buntkowsky, H.-H. Limbach in *Dihydrogen Transfer and Symmetry: The Role of Symmetry on the Chemistry of Dihydrogen Transfer in the Light of NMR Spectroscopy, Vol. 2* (Eds.: J. P. Hynes, J. P. Klinman, H.-H. Limbach, R. L. Schowen), Wiley-VCH, Weinheim, **2006**, pp. 639 – 682.
[96] B. Chaudret in *Synthesis and Surface Reactivity of Organometallic Nanoparticles, Vol. 16*, Springer, Berlin, Heidelberg, **2005**, pp. 233 – 259.
[97] K. Philippot, B. Chaudret, *C. R. Chim.* **2003**, *6*, 1019 – 1034.
[98] T. Pery, K. Pelzer, G. Buntkowsky, K. Philippot, H. H. Limbach, B. Chaudret, *ChemPhysChem* **2005**, *6*, 605 – 607.
[99] J. García-Antón, M. R. Axet, S. Jansat, K. Philippot, B. Chaudret, T. Pery, G. Buntkowsky, H. H. Limbach, *Angew. Chem.* **2008**, *120*, 2104 – 2108; *Angew. Chem. Int. Ed.* **2008**, *47*, 2074 – 2078.
[100] F. Schröder, D. Esken, M. Cokoja, M. W. E. van den Berg, O. I. Lebedev, G. van Tendeloo, B. Walaszek, G. Buntkowsky, H.-H. Limbach, B. Chaudret, R. A. Fischer, *J. Am. Chem. Soc.* **2008**, *130*, 6119 – 6130.

[101] B. Walaszek, Y. P. Xu, A. Adamczyk, H. Breitzke, K. Pelzer, H. H. Limbach, J. L. Huang, H. X. Li, G. Buntkowsky, *Solid State Nucl. Magn. Reson.* **2009**, *35*, 164 – 171.
[102] L. A. Truflandier, I. Del Rosal, B. Chaudret, R. Poteau, I. C. Gerber, *ChemPhysChem* **2009**, *10*, 2939 – 2942.
[103] I. del Rosal, L. Truflandier, R. Poteau, I. C. Gerber, *J. Phys. Chem. C* **2011**, *115*, 2169 – 2178.
[104] K. Honkala, A. Hellman, I. N. Remediakis, A. Logadottir, A. Carlsson, S. Dahl, C. H. Christensen, J. K. Nørskov, *Science* **2005**, *307*, 555 – 558.

Received: February 25, 2013
Published online on May 9, 2013